Research Square

Preprints are preliminary reports that have not undergone peer review.
They should not be considered conclusive, used to inform clinical practice,
or referenced by the media as validated information.

Spatiotemporal Variation of Particulate Matters (PM2.5 and PM10) and Their Relationship with Meteorological Conditions in North India during 2018-2025

Gaurav Singh
India Meteorological Department
M. P. Raju
prmade@amity.edu

Amity University Uttar Pradesh (AUUP)
V. K. Soni
India Meteorological Department
Chinmay Jena
India Meteorological Department
Suman Gurjar
India Meteorological Department

Research Article

Keywords: PM2.5, PM10, North India, Spatio-temporal analysis, Mann-Kendall test, Pearson correlation analysis

Posted Date: November 23rd, 2026

DOI: https://doi.org/10.21203/rs.3.rs-11243817/v1

License: This work is licensed under a Creative Commons Attribution 4.0 International License.
Read Full License

Additional Declarations: No competing interests reported.

Spatiotemporal Variation of Particulate Matters ($PM_{2.5}$ and PM_{10}) and Their Relationship with Meteorological Conditions in North India during 2018-2025

Gaurav Singh[1], M.P. Raju[2]*, V.K. Soni[1], Chinmay Jena[1], Suman Gurjar[1]

[1] India Meteorological Department, Ministry of Earth Sciences, New Delhi, India

[2] Department of Climate Change and Environmental Sustainability, Amity Institute of Environment and Sustainability, Amity University Uttar Pradesh (AUUP), Noida, India.

Abstract

Fine ($PM_{2.5}$) and coarse (PM_{10}) particulate matter air pollution in northern India display considerable spatiotemporal variability and seasonality, making it challenging to interpret the Spatio-temporal trend patterns considering the changes in meteorological conditions. The objective of this study is to investigate the spatiotemporal variations of $PM_{2.5}$ and PM_{10} in 81 cities from 2018 to 2025 and their relationship with the meteorological conditions in 37 cities with available meteorology data. Using Sens slope and Mann-Kendall test, city-level annual and seasonal trend was analyzed; while using station fixed effects panel regression and Pearson correlation analysis was performed on the relationship between particulate pollution and meteorology. The network wide multi-year average concentration of $PM_{2.5}$ and PM_{10} were 62.7 μg/m³ and 130.0 μg/m³, respectively, where high values of particulates were found in Delhi-NCR and adjoining regions of Uttar Pradesh and Haryana. Annual concentrations of $PM_{2.5}$ were higher in post-monsoon (90.0 μg/m³) and winter (87.0 μg/m³) than the monsoon period (36.0 μg/m³). Both particulates were inversely correlated with wind speed and precipitation. Relative humidity showed contrasting seasonal correlation with $PM_{2.5}$, positively associated with it in winter (β=0.178), while negatively in monsoon (β= -0.290).

Keywords: $PM_{2.5}$; PM_{10}; North India; Spatio-temporal analysis; Mann-Kendall test; Pearson correlation analysis

Corresponding Author:

M.P. Raju (prmade@amity.edu)

ORCID iDs: 0000-0002-2090-2285 (M.P. Raju)

1. Introduction

Air pollution is a major global public health concern and an important contributor to premature mortality worldwide. Nearly 99% of the global population is exposed to air pollution levels that exceed the World Health Organization (WHO) air quality guidelines (WHO 2022; Venkatesan, 2016; Landrigan, 2017). It causes over 6.5 million deaths annually 11.65% of global fatalities (Landrigan et al., 2022; Ritchie & Roser, 2017) and generates economic losses of approximately $8.1 trillion, or 6.1% of world GDP (World Bank 2022). Among atmospheric pollutants, particulate matter ($PM_{2.5}$ and PM_{10}) poses the greatest health and environmental risk due to its ability to penetrate the respiratory system, contribute to cardiovascular disease, diabetes, and neurological disorders, and disrupt ecosystems and food security (Di et al. 2020; Kumar et al. 2022; He et al. 2022; Guo et al. 2023d; Guo et al. 2024a; Ramadan et al. 2025). Exposure is highly unequal, with low-income and densely populated urban communities bearing a disproportionate burden due to traffic density, weak regulatory enforcement, and limited pollution control infrastructure (Zhong et al. 2023; Ngo et al. 2019; Mani et al. 2020). South Asia is particularly affected: $PM_{2.5}$ exposure was identified as the third-leading mortality risk factor in the region in 2015, with India alone recording an estimated 1.1 million $PM_{2.5}$ related deaths annually (Krishna et al. 2017; David et al. 2019; Shi et al. 2018; Cao et al. 2013).

In response, the Government of India launched the National Clean Air Programme (NCAP) in January 2019, targeting a 20 - 30% reduction in $PM_{2.5}$ and PM_{10} concentrations across 122–131 non-attainment and million-plus cities by 2024 relative to a 2017 baseline; this target was later revised upward to a 40% reduction by 2026 (MoEFCC 2019; CPCB 2026). Progress-tracking data indicate that the burden of non-attainment remains heavily concentrated in the Indo-Gangetic Plain (IGP) of 61 IGP cities with adequate monitoring coverage, 47 continue to exceed national ambient air quality standards, with Bihar, Rajasthan, and Uttar Pradesh showing the highest rates of non-compliance (CPCB 2026). This makes the IGP not only the region of greatest public-health concern

but also the most policy-relevant test bed for evaluating whether and where air quality is genuinely improving.

A growing body of atmospheric research suggests that meteorology, independent of emissions policy, plays a decisive role in that trajectory. Paulot et al. 2022, found that $PM_{2.5}$ concentrations in the IGP rise systematically as near-surface wind speed declines, and that continued CO_2 driven weakening of regional winds is likely to worsen wintertime air quality even without any change in emissions. Consistent with this, Xie et al. 2024, showed that around 30% of the annual $PM_{2.5}$ improvement observed in India's non-attainment cities since 2017 and nearly half of the reduction recorded during the heavily polluted winter months which was attributable to favourable meteorological conditions rather than to emissions abatement, and cautioned that such conditions are unlikely to persist as the climate continues to warm. Together, these findings indicate that improvements related to the NCAP targets cannot be understood reliably without making the meteorological versus anthropogenic differentiation, a factor that has not been considered to this point in multi-city multi-year analysis.

Even taking into account the severity of pollution in India, there are certain gaps in the research related to the PM changes at the scale level. The majority of the research conducted focuses on studying individual megacities (or short periods such as Delhi lockdown) without paying sufficient attention to the multi-station analysis covering the whole IGP over a number of years before and after the implementation of the NCAP policy. There is still a shortage of comprehensive studies, which analyze the relationship between particulate concentrations and the meteorology over larger networks of cities. Most of the studies cover only few locations while ignoring the heterogeneity of the region. Additionally, it should be noted that air pollution research in India is focused primarily on the IGP because of its severity, which means that the methodology related to the integration of trend detection (e.g. significance testing) and meteorological attribution at scale level has not been developed yet.

This study investigates the spatial and temporal variation of $PM_{2.5}$ and PM_{10} concentrations across North India using ground-based and meteorological observations from 2018–2025. The specific objectives are to: (1) characterize spatiotemporal $PM_{2.5}$ and PM_{10} trends across 81 North Indian cities; (2) assess regional changes and identify cities most severely affected by particulate pollution; (3) analyse long-term meteorological trends (wind speed, temperature, pressure, humidity, precipitation) across 37 cities with available meteorological records; and (4) quantify the relative contribution of each meteorological factor to particulate variability - providing an evidence base for targeted, city- and season-specific air quality management strategies across the IGP.

2. Methodology

2.1 Study Area

This study covers eleven states of northern and central India (20°N - 33°N and 68°E - 89°E) (**Figure 1**). The study domain includes Punjab, Haryana, Delhi (NCT), Uttar Pradesh, Bihar, West Bengal, Jharkhand, Chhattisgarh, Madhya Pradesh, Rajasthan, and Gujarat together covering over 2.1 million km² and home to approximately 800 million people about 60% of India's population. Encompassing Punjab, Haryana, Delhi, Uttar Pradesh, Bihar, West Bengal, Jharkhand, Chhattisgarh, Madhya Pradesh, Rajasthan, and Gujarat, the multi-state domain captures the full spatial gradient of particulate pollution across the IGP and adjoining regions, which rank among the world's most polluted airsheds (Kumar et al. 2021; Kuttippurath et al. 2022). The ground-truth particulate data is obtained from the Central Pollution Control Board's (CPCB) - CAAQMS network, with the region's non-attainment status of the region concerning India's NCAP reflecting its policy implications (CAQM 2023; Sharma et al. 2025). The physical geography plays a crucial role in the pollution distribution; with the Himalayan mountain range preventing further diffusion of pollutants and keeping them trapped in IGP (Dumka et al. 2021; Raul et al. 2025) and the Thar Desert serving as a source of wind borne dust for western states. The region comprises of four different climatic zones,

where the Indian Summer Monsoons (ISM) results in wet scavenging during June - September, followed by a sharp post-monsoon and winter peak driven by atmospheric stagnation, thermal inversions, low boundary layers, and biomass burning (Patel et al. 2022; ICIMOD 2024).

The area is characterized by highly concentrated local pollution sources, such a vehicular emissions, industrial activities, thermal electricity production, mining, construction dust, and agricultural residue burning incidents. Agricultural burning of post-monsoon paddy residues in the west IGP is common in Punjab and Haryana (Singh et al. 2022; Sharma et al. 2025), while Delhi has a problem of excessive $PM_{2.5}$ concentrations surpassing national and WHO standards (Lakra & Avishek 2024; Sharma et al. 2025). The high concentration in Uttar Pradesh and Bihar are caused by high population density, intense traffic, brick kilns, and biomass burning (Sharma et al. 2024; Wei et al. 2024). On the eastern side of the study area, industrial and urban centres of highly polluted areas are located in Kolkata and Asansol (Chatterjee et al. 2025), while Jharkhand and Chhattisgarh regions have significant industrial and mining emissions in the Jharia, Bokaro, and Korba areas (Mohammad et al. 2025; Naskar et al. 2025). Finally, Madhya Pradesh, Rajasthan, and Gujarat exhibit elevated particulate levels shaped by mineral mining, thermal power plants, rapid industrialization, and dust-dominated arid regimes (Kumar et al. 2018; Sharma et al. 2024).

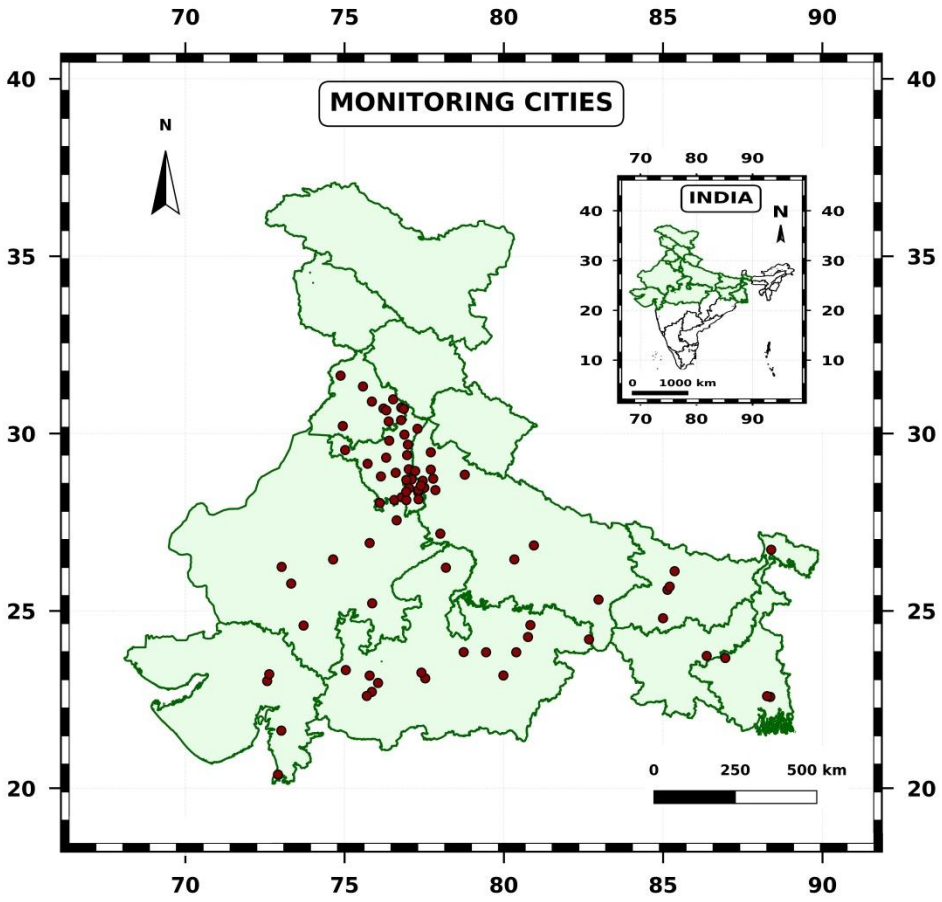

Figure 1. *Map of the study area states along with the 81 cities considered in the study.*

2.2 Data Acquisition

2.2.1 Pollutant Data

Hourly $PM_{2.5}$ and PM_{10} data (2018–2025) were obtained from CPCB's online portal (https://cpcb.nic.in/), sourced from its national CAAQMS network, using the gravimetric measurement method (Kamyotra et. al. 2011). Ambient $PM_{2.5}$ and PM_{10} concentrations were measured with the BAM-1022 Beta Attenuation Mass Monitor (Met One Instruments Inc.), which draws air through a filter tape exposed to beta rays from a Carbon-14 source, converting attenuation into mass concentration (MetOne, 2020). $PM_{2.5}$ and PM_{10} fractions are separated using size-selective inlets (a sharp-cut cyclone/VSCC for $PM_{2.5}$, a PM_{10} selective inlet for PM_{10}), via inlet-swapping or parallel units.

Data collection followed CPCB's National Air Monitoring Programme (NAMP) protocols, with instrument calibration per U.S. EPA guidelines (2023) and Quality Assurance/Quality Control (QA/QC) procedures detailed in CPCB (Bhawan & Nagar 2020) and at https://cpcb.nic.in/quality-assurance-quality-control/.

2.2.2 Meteorological Data

Hourly meteorological data (2018–2025) of Temperature (Temp), Relative Humidity (RH), Wind Speed (WS), Atmospheric Pressure (AP), and Precipitation (PPT) were sourced from the IMD Data Supply Portal (https://dsp.imdpune.gov.in/), matched temporally to the PM dataset which gives 37 cities data comprising both PM's and meteorological data. Where station-level data were unavailable, the nearest IMD observatory was used as a proxy. Data were quality-checked and aggregated to monthly and seasonal scales for use as explanatory variables in subsequent trend and panel regression analyses.

2.3 Statistical and Analytical Methods

2.3.1 Data Pre-processing

Hourly $PM_{2.5}$ and PM_{10} concentrations from 81 cities CPCB stations and hourly meteorological records (Temp, RH, WS, AP, and PPT) from the IMD Data Supply Portal for the 37 cities were aggregated to daily, monthly, and seasonal means for the period January 2018–December 2025. Missing values due to instrument outages or data transmission errors were identified and removed rather than imputed to avoid the creation of spurious trend patterns. Seasons were defined as Winter (December–February), Pre-monsoon (March–May), Monsoon (June–September), and Post-monsoon (October–November), consistent with standard classification for the Indian subcontinent. All meteorological and pollutant records were matched by station and date prior to trend and regression analysis to ensure temporal alignment between the two datasets.

2.3.2 Data Quality Control

Quality-controlled $PM_{2.5}$ and PM_{10} observations were obtained from CPCB's Continuous Ambient Air Quality Monitoring Stations (CAAQMS) network across 81 cities in North India. Details of instrument calibration and the standard QA/QC procedures followed by CPCB are available at https://cpcb.nic.in/quality-assurance-quality-control/. In addition to CPCB's automated quality control, an additional filtering step was applied to remove spurious observations, following the approach adopted by Jena et al. (2021) for $PM_{2.5}$ data over Delhi: $PM_{2.5}$ and PM_{10} measurements exceeding 1000 $\mu g/m^3$, as well as values corresponding to documented instrument malfunction, were excluded from the dataset as physically implausible or unreliable.

Meteorological observations (Temp, RH, WS, AP, and PPT) were similarly quality controlled prior to analysis. Records with missing values were excluded rather than imputed, to avoid introducing artificial trend structure into the subsequent Sen's slope and Mann-Kendall analyses. Extreme outlier values which were impossible to obtain physically and were outside the normal range of climate expected for each of the variables were eliminated for all the five meteorological variables from each station, making sure that the data set finally used for trend analysis was not due to sensor errors.

2.3.3 Spatial Distribution Mapping

Average $PM_{2.5}$ and PM_{10} concentrations on an annual basis and during each season were estimated city-wise using all the data available for each station in the period of 2018-2025 and during each meteorological season individually. These averages for each station were presented on a geographically located map in the form of bubbles whose size and color would depend on the concentration classes.

2.3.4 Sen's Slope Trend Estimation

The magnitude and direction of long-term trends in annual and seasonal $PM_{2.5}$ and PM_{10} concentrations at each city were quantified using the Theil–Sen slope estimator (Theil 1950; Sen 1968), a non-parametric method robust to outliers and non-normal data distributions. For a time series of n observations, the slope was calculated as the median of all pairwise slopes:

Sen's Slope Estimator

$$\beta = \text{Median}\left(\frac{x_j - x_i}{j - i}\right), \forall\, i < j \quad \ldots \quad (1)$$

Where:

- β = Sen's slope estimate (rate of change per unit time)
- x_j, x_i = data values (PM concentration or meteorological variable) at times j and i, respectively
- j, i = time indices, with j > i

A positive β indicates an increasing trend over time; a negative β indicates a decreasing trend. The magnitude of β represents the rate of change per year.

A positive slope indicates an increasing concentration trend over time, while a negative slope indicates a decreasing trend; the absolute magnitude reflects the rate of change per year. This procedure was applied independently to each city's annual mean series and to each of the four seasonal mean series, yielding city-specific and season-specific slope estimates for both pollutants.

2.3.5 Mann–Kendall Significance Testing

The statistical significance of each Sen's slope trend was evaluated using the non-parametric Mann–Kendall (MK) test (Mann 1945; Kendall 1975), which assesses the presence of a monotonic trend without assuming an underlying data distribution. The test statistic S was computed as:

Mann–Kendall Test Statistic

$$S = \sum_{i=1}^{n-1} \sum_{j=i+1}^{n} \operatorname{sgn}\left(x_j - x_i\right) \quad \ldots (2)$$

$$\operatorname{sgn}\left(x_j - x_i\right) = \begin{cases} +1, & \text{if } \left(x_j - x_i\right) > 0 \\ 0, & \text{if } \left(x_j - x_i\right) = 0 \\ -1, & \text{if } \left(x_j - x_i\right) < 0 \end{cases}$$

Where:

- S = Mann–Kendall test statistic
- n = number of data points in the time series
- x_i, x_j = sequential data values, with j > i
- sgn(·) = sign function

The variance of S and the corresponding standardized Z-statistic are then used to determine trend significance at the chosen confidence level ($p < 0.05$ in this study). Trends were classified into four categories i.e., Significant Decreasing, Non-significant Decreasing, Non-significant Increasing, and Significant Increasing based on the sign of the Sen's slope and the p-value of the corresponding MK statistic. This classification was applied at the annual scale (per city) and the seasonal scale (per city–season combination), enabling identification of cities and seasons with statistically robust improvement or deterioration in air quality, as distinct from short-term fluctuation.

2.3.6 Meteorological Trend Analysis

Long-term trends in the five meteorological variables Temp, RH, WS, AP, and PPT were assessed at each of the 37 stations with complete meteorological records using the same Sen's slope and Mann–Kendall framework described in above section, applied separately at the annual scale and for each of the four seasons. A positive slope denotes an increasing trend in the meteorological variable over the study period, and a negative slope a decreasing trend; the magnitude reflects the rate of annual change. Results were mapped spatially by station to identify regional patterns of change, particularly the wind-stilling and humidity-increase trends.

2.3.7 Panel Regression Analysis

To quantify the relationship between meteorological conditions and particulate concentrations while controlling for station-level heterogeneity, a cross-sectional fixed-effects panel regression model was estimated using monthly station-level data. The model was specified as:

Panel Regression Model (Fixed-Effects)

$$Y_{it} = \alpha_i + \beta_1 WS_{it} + \beta_2 Pre_{it} + \beta_3 AP_{it} + \beta_4 Tem_{it} + \beta_5 RH_{it} + \varepsilon_{it} \quad \ldots (3)$$

Where:

- Y_it = concentration of PM2.5 or PM10 at station *i* in month *t*
- α_i = station-specific fixed effect
- WS_it, Pre_it, AP_it, Tem_it, RH_it = wind speed, precipitation, atmospheric pressure, temperature, and relative humidity at station *i* in month *t*, respectively
- β_1–β_5 = estimated regression coefficients for each meteorological variable
- ε_it = error term

where Y_it is the concentration of $PM_{2.5}$ or PM_{10} at station i in month t; α_i denotes the station-specific fixed effect; Temp, RH, WS, AP, and PPT and ε_it is the error term. The model was estimated separately for the annual (all-years-combined) dataset and for each of the four seasonal

subsets, using ordinary least squares (OLS) with station fixed effects. Model significance was assessed using the F-test, and the significance of individual coefficients was assessed using the t-test. Both unstandardized coefficients (in original physical units) and standardized coefficients (β, for cross-variable comparability) were reported, and R^2 was used to evaluate overall model fit.

2.3.8 Pearson Correlation Analysis

To complement the panel regression and examine bivariate associations independent of its fixed-effects structure, zero-order Pearson product-moment correlation coefficients (r) were computed between $PM_{2.5}$, PM_{10}, and each of the five meteorological variables, using the full pooled daily observation dataset. Correlations were computed separately at the annual scale and within each of the four meteorological seasons to capture season-dependent shifts in the strength and direction of pollutant–meteorology relationships. Statistical significance of each correlation coefficient was assessed at $p < 0.001$, and inter-variable correlations among the meteorological parameters themselves (e.g., pressure–temperature) were also examined to interpret the physical consistency of the regression.

3. Results

3.1 Spatio-Temporal Distribution of $PM_{2.5}$ and PM_{10} Concentrations in North Indian Cities

The spatial distribution maps of annual mean $PM_{2.5}$ (**Figure 2a**) and PM_{10} (**Figure 2b**) concentrations (2018–2025) across 81 monitored cities show a strongly clustered pollution pattern centred on the IGP. Both pollutants peak sharply (corresponding to the 161–200+ $\mu g/m^3$ classes) between roughly 28 – 30° N and 76 – 79° E covering Delhi-NCR and adjoining districts of western Uttar Pradesh and Haryana - with Greater Noida, Ghaziabad, Baghpat, Bhiwadi, Noida, Faridabad, and Delhi recording the highest values. Outside this cluster, concentrations decrease significantly in Rajasthan, Madhya Pradesh, Bihar, West Bengal, and northeastern states where small to medium-sized markers occur (mostly in the 0–100 $\mu g/m^3$ range), with some moderate to large sized hot spots

appearing at the eastern edge of the IGP (such as Bihar-WB state boundary) and central Indian regions (like Singrauli). Similar distribution for both size fractions indicates a common regional source and meteorological control in the IGP region.

The multi-year combined mean was 130.0 μg/m^3 for PM_{10} and 62.7 μg/m^3 for $PM_{2.5}$ both far exceeding India's NAAQS (PM_{10}: 60; $PM_{2.5}$: 40 μg/m^3) and WHO guidelines (PM_{10}: 15; $PM_{2.5}$: 5 μg/m^3). The highest long-term mean PM_{10} concentrations were recorded in the National Capital Region (NCR) and nearby cities of Uttar Pradesh and Haryana. Greater Noida (218.0 μg/m^3), Ghaziabad (217.0 μg/m^3), Baghpat (210.9 μg/m^3), Bhiwadi (210.0 μg/m^3), Noida (206.0 μg/m^3), Faridabad (202.3 μg/m^3), and Delhi (198.3 μg/m^3) exhibited the most severely elevated PM_{10} levels. Lowest levels of PM_{10} were registered in the smaller cities of Maihar, Damoh, Gaya, and Gandhinagar that are not part of the core of IGP, but an exceptionally high level of $PM_{2.5}$ in Sirsa with low PM_{10} (**Table 1**) suggests sensor malfunctioning or specific sources of fine particulate matter. For $PM_{2.5}$, the spatial pattern largely mirrored that of PM_{10}, with Ghaziabad (103.4 μg/m^3), Moradabad (101.4 μg/m^3), Bhiwadi (98.4 μg/m^3), Baghpat (96.8 μg/m^3), Noida (93.7 μg/m^3), Gurugram (91.3 μg/m^3), Delhi (91.0 μg/m^3), and Greater Noida (89.6 μg/m^3) recording the highest values. The lowest $PM_{2.5}$ values were found in Maihar (27.1 μg/m^3), Satna (31.4 μg/m^3), Sagar (32.1 μg/m^3), Gandhinagar (32.6 μg/m^3), and Damoh (33.2 μg/m^3).

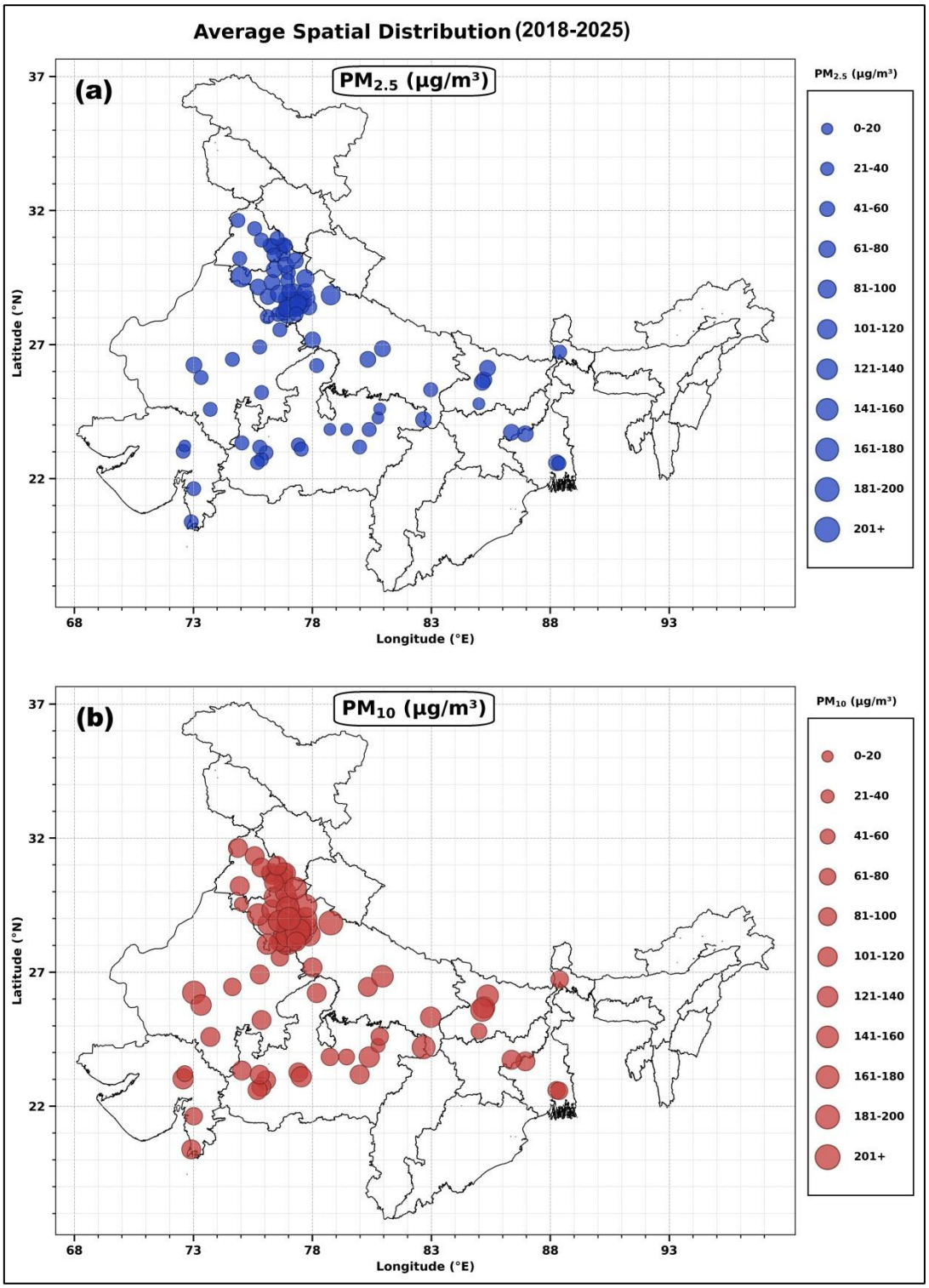

Figure 2: *Spatial plots of city-wise PM averages - a) $PM_{2.5}$, b) PM_{10}*

Table 1: Multi-year Annual Mean PM Concentrations for Selected Cities-Highest and Lowest Cities

City	State	PM_{10} (µg/m^3)	$PM_{2.5}$ (µg/m^3)
Greater Noida	Uttar Pradesh	218.0	89.6
Ghaziabad	Uttar Pradesh	217.0	103.4
Bhiwadi	Rajasthan	210.0	98.4
Noida	Uttar Pradesh	206.0	93.7
Faridabad	Haryana	202.3	86.5
Delhi	Delhi (NCT)	198.3	91.0
Moradabad	Uttar Pradesh	195.5	101.4
Gurugram	Haryana	176.8	91.3
Singrauli	Madhya Pradesh	177.9	77.0
Patna	Bihar	167.1	74.7
Jodhpur	Rajasthan	160.8	73.2
Gandhinagar	Gujarat	78.1	32.6
Damoh	Madhya Pradesh	63.5	33.2
Maihar	Madhya Pradesh	51.0	27.1
Combined mean (81 cities)	—	**130.0**	**62.7**

Seasonally, concentrations followed a consistent cycle across all cities: highest in post-monsoon and winter, intermediate in pre-monsoon, and lowest in monsoon (**Figure S1**, **Table S1**). The post-monsoon season recorded the highest average PM_{10} (172.1 µg/m^3) and $PM_{2.5}$ (90.0 µg/m^3), followed closely by winter (PM_{10}: 163.9 µg/m^3; $PM_{2.5}$: 87.0 µg/m^3). Pre-monsoon levels were intermediate (PM_{10}: 133.9 µg/m^3; $PM_{2.5}$: 56.4 µg/m^3), while the monsoon season exhibited the lowest concentrations (PM_{10}: 80.3 µg/m^3; $PM_{2.5}$: 36.0 µg/m^3).This pattern reflects well-established drivers - post-monsoon and winter bring stable boundary layers, reduced vertical mixing, intensified stubble burning in Punjab and Haryana, and increased biomass-based domestic heating, while monsoon rainfall drives wet scavenging and turbulent dispersion that sharply lowers PM loads

(Kumar et al. 2015; Pant et al. 2017; Srivastava et al. 2014). At the city level, Delhi's $PM_{2.5}$ reached ~125–154 μg/m^3 across post-monsoon and winter, consistent with local emissions compounded by regional stubble-burning transport (Cusworth et al. 2018), while NCR-periphery cities - Ghaziabad, Noida, Meerut, Bulandshahr - saw winter PM_{10} frequently exceed 250–390 μg/m^3.

Together, these spatial and seasonal patterns confirm the IGP as a persistent particulate hotspot, driven by agricultural residue burning, rapid urbanisation, traffic density, industrial and brick-kiln emissions, and meteorological conditions favouring pollutant accumulation - low wind speeds, temperature inversions, and elevated aerosol optical depth (Balakrishnan et al. 2019; Guttikunda & Gurjar 2012; Pant et al. 2017).

3.2 Trend Classification of $PM_{2.5}$ and PM_{10}

3.2.1 Annual Spatial Trends

Figure 3a ($PM_{2.5}$) and **Figure 3b** (PM_{10}) represents the direction and magnitude of temporal trends in annual concentrations for each city using Sen's Slope Estimator, a robust non-parametric measure of trend magnitude (Sen 1968; Theil 1950). For PM_{10}, slopes in the 81 cities varied from -33.4 (Rohtak) and +16.0 μg/m^3/year (Bahadurgarh), with a median value of -2.3, revealing a declining trend. Cities witnessing the highest decreases in PM_{10} concentrations included Rohtak (-33.4), Kanpur (-27.3), Varanasi (-26.4), Hapur (-23.8), Agra (-22.6), Bhiwadi (-17.2), and Lucknow (-16.7), all significant urban centers in UP, Rajasthan, and Haryana. Only 13 cities (16.3%) exhibited positive slopes, such as Bahadurgarh (+16.0), Dharuhera (+9.8), Rupnagar (+1.5), Chandigarh (+2.7), and Ludhiana (+1.4), that revealed local increases probably due to increased industry, population expansion, or lack of emission controls. For $PM_{2.5}$, slopes varied between -12.4 (Hapur) and +10.2 μg/m^3/year (Bahadurgarh), with a median of -1.5. Steep decrease were observed in Hapur (-12.4), Varanasi (-11.6), Kanpur (-9.2), Meerut (-8.5), Agra (-8.4), and Ghaziabad (-8.0), all located in UP, suggesting cumulative effects of NCAP interventions, LPG adoption over solid fuels, and post-COVID industrial shifts. Positive slopes appeared in 26 of 81 cities (32.1%), including

Bahadurgarh (+10.2), Bhiwani (+5.9), Dharuhera (+6.6), Hajipur (+4.5), Panchkula (+4.4), and Kota (+2.4), showing fine particle levels are still rising in a notable minority of cities.

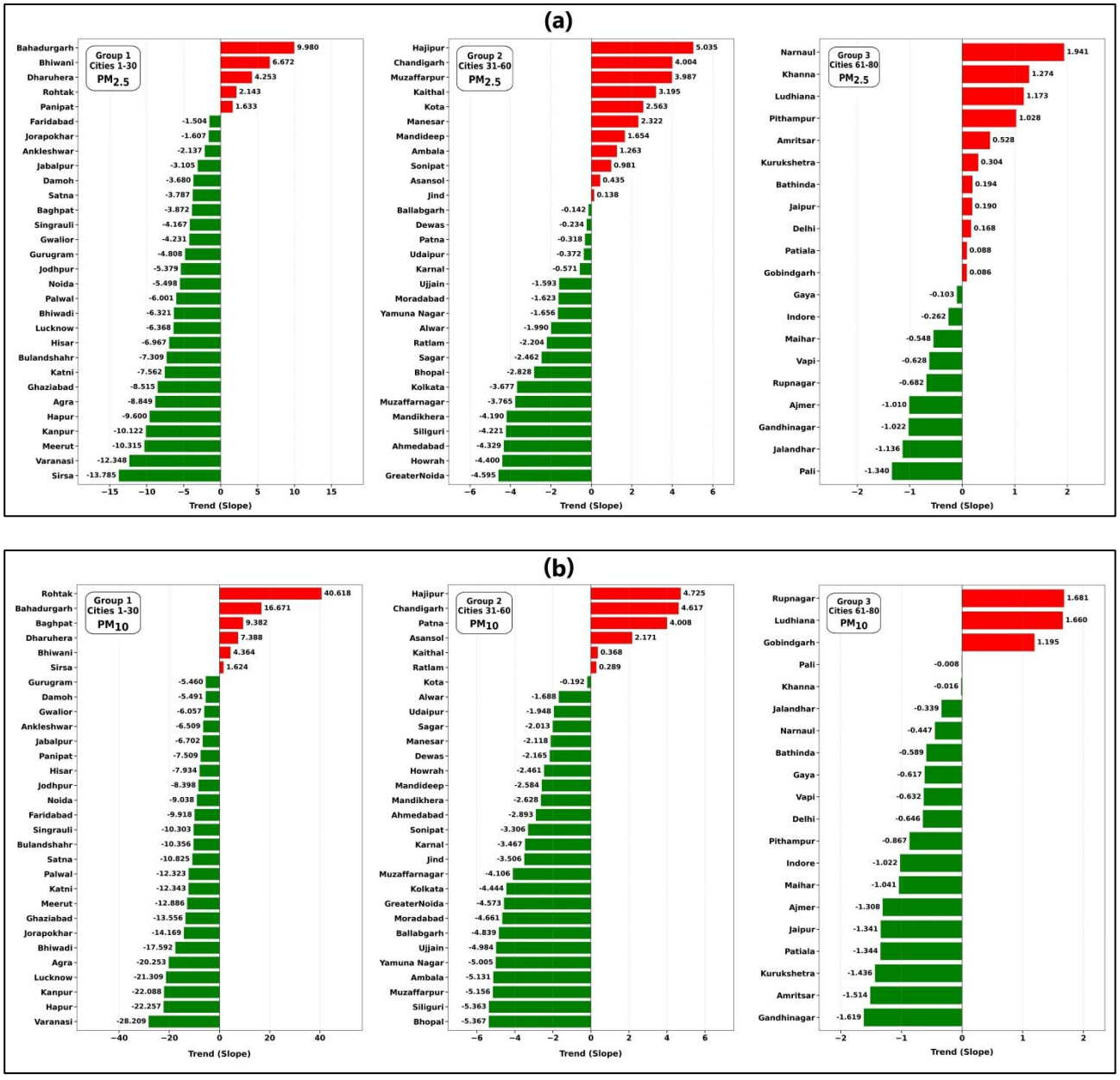

Figure 3 Annual trend of $PM_{2.5}$ (Top Panel) and PM_{10} (Bottom Panel)

3.2.2 Seasonal Spatial Trends

Seasonal Sen's slope analysis from **Figure S2 and Figure S3** showed the strongest, most widespread decreases in post-monsoon and winter for PM_{10}, and in winter and monsoon for $PM_{2.5}$. $PM_{2.5}$ (**Figure S2**) showed significant decreasing trends predominantly in winter and monsoon.

Specifically, 26 city-season combinations showed significant winter PM_{10} decreases, and 15 showed significant post-monsoon PM_{10} decreases. For $PM_{2.5}$, winter recorded 26 significant decreases, monsoon 17, and post-monsoon 16. Pre-monsoon trends were comparatively fewer (PM_{10}: 1 significant decrease; $PM_{2.5}$: 7 significant decreases), reflecting lower baseline concentrations and weaker pollutant accumulation processes during that period. Spatially, Haryana cities (Faridabad, Gurugram, Panipat, Palwal, Rohtak, Yamuna Nagar, Kaithal, Ambala) and Madhya Pradesh cities (Bhopal, Damoh, Jabalpur, Katni) showed pervasive winter and post-monsoon PM_{10} declines (**Figure S3**). Delhi showed a significant monsoon $PM_{2.5}$ decrease (slope = -0.38 $\mu g/m^3$/year, p = 0.022), while Ahmedabad declined significantly across all four seasons (slopes: -0.53 to -1.32 $\mu g/m^3$/year). These patterns likely reflect both targeted measures (Delhi's odd-even scheme, crop-burning bans, coal plant shutdowns) and broader structural shifts in energy and transport sectors.

3.2.3 Mann-Kendall Test for Significance and Non-Significance

The statistical significance of temporal trends was assessed using the non-parametric Mann–Kendall (MK) test (Mann 1945; Kendall 1975), a non-parametric rank-based method widely used in environmental trend detection due to its robustness against non-normality, missing data, and seasonality effects (Hirsch et al. 1982; Yue et al. 2002) (**Figure 4**). Trends were classified into four categories: Significant Decreasing ($p < 0.05$, negative slope), Non-significant Decreasing, Non-significant Increasing, or Significant Increasing (**Table 2**).

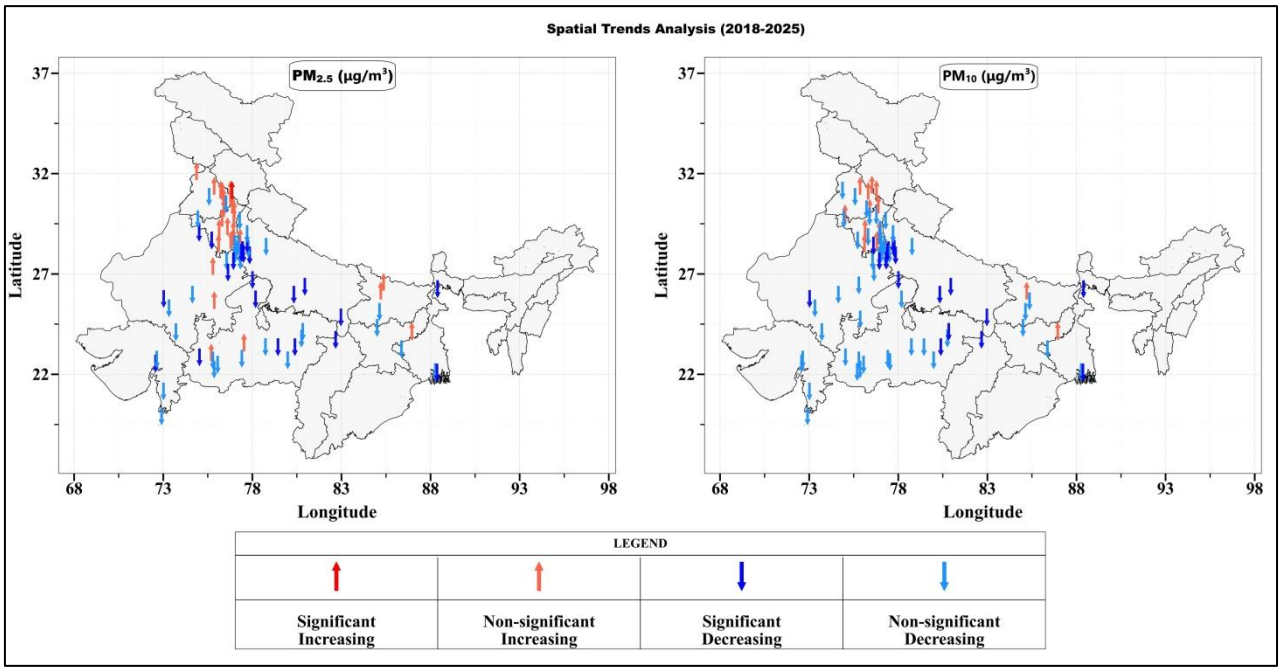

Figure 4: *Categorical map of significant vs. non-significant annual MK trends for $PM_{2.5}$ and PM_{10}*

As shown in **Table 2,** 22 of 81 cities (27.2%) showed significant decreasing $PM_{2.5}$ trends, against just one significant increase (Panchkula, Haryana: +4.4 µg/m^3/year, p = 0.041). Most cities (71.6%) showed non-significant trends (32 decreasing, 26 increasing). For PM_{10}, 18 of 80 cities (22.5%) declined significantly - led by Varanasi (-26.4, p = 0.0005), Kanpur (-27.3, p = 0.012), Hapur (-23.8, p = 0.014), Agra (-22.6, p = 0.046), Lucknow (-16.7, p = 0.013), Ghaziabad (-13.3, p = 0.006), and Meerut (-12.9, p = 0.009); no city showed a significant PM_{10} increase, though Haryana (Bahadurgarh, Bhiwani, Dharuhera) and Punjab (Ludhiana, Chandigarh, Rupnagar, Khanna) showed non-significant upward slopes. Significant $PM_{2.5}$ declines clustered in Uttar Pradesh (Varanasi, Kanpur, Lucknow, Ghaziabad, Noida, Bulandshahr, Meerut, Greater Noida, Agra) and Madhya Pradesh (Singrauli, Katni, Gwalior, Ratlam, Damoh), with further cases in Rajasthan, Gujarat, Haryana, and West Bengal.

Table 2: Summary of Mann-Kendall Trend Categories for Annual PM_{10} and $PM_{2.5}$ (* Number of Cities)

Trend Category	PM_{10}*	PM_{10} (%)	$PM_{2.5}$ *	$PM_{2.5}$ (%)
Significant Decreasing	18	22.5	22	27.2
Non-significant Decreasing	49	61.3	32	39.5
Non-significant Increasing	13	16.3	26	32.1
Significant Increasing	0	0.0	1	1.2
Total	**80**	100	**81**	100

As shown in **Table S2,** declines were most frequent in winter and post-monsoon seasons the periods of peak pollution for both pollutants also shown as figures, i.e., $PM_{2.5}$ (**Figure S4**) and PM_{10} (**Figure S5**). Winter alone accounted for 26 significant decreases each for PM_{10} and $PM_{2.5}$, with Rohtak showing the steepest PM_{10} decline (-14.5 $\mu g/m^3$/year, $p \approx 0$) and UP/West Bengal cities (Varanasi, Kanpur, Lucknow, Howrah, Kolkata, Siliguri) leading $PM_{2.5}$ improvements. Post-monsoon PM_{10} declines were concentrated in Haryana (Faridabad, Gurugram, Kaithal, Palwal, Panipat, Yamuna Nagar) and Madhya Pradesh (Bhopal, Jabalpur, Katni). Monsoon $PM_{2.5}$ declined significantly in 17 cities, including Delhi (-0.38, $p = 0.022$) and Ahmedabad (-0.53, $p = 0.013$), modest slopes, but statistically meaningful even in the wet season. Non-significant increasing trends persisted in several Haryana and Punjab cities across seasons, pointing to localized industrial/urban expansion offsetting regional gains.

Taken together, the Mann-Kendall trend analysis demonstrates that air quality in northern India is predominantly improving - with nearly half of all cities showing some form of decreasing PM_{10} and $PM_{2.5}$ trend - yet the pace of improvement is uneven across the region. The high-pollution IGP core (Delhi, NCR, Lucknow, Kanpur, Varanasi belt) shows significant reductions, likely owing to concentrated policy action, while several Haryana and Punjab cities exhibit non-significant or even

positive trends. These findings underscore the need for city-specific, spatially disaggregated air quality management strategies rather than broad regional approaches.

Collectively, these finding suggests a reasonable correlation between these declines and concurrent efforts which include: NCAP (2019, targeting 20-30% PM reduction in 132 cities by 2024), PMUY efforts for LPG use, BS-VI emission standards (April 2020), the 2020 lockdown for COVID-19, and CAQM initiatives in NCR (CPCB 2019; MoEFCC 2019; Sharma et al. 2021).

3.3 Spatiotemporal Trends in Meteorological Variables (2018–2025)

3.3.1 Annual meteorological trends

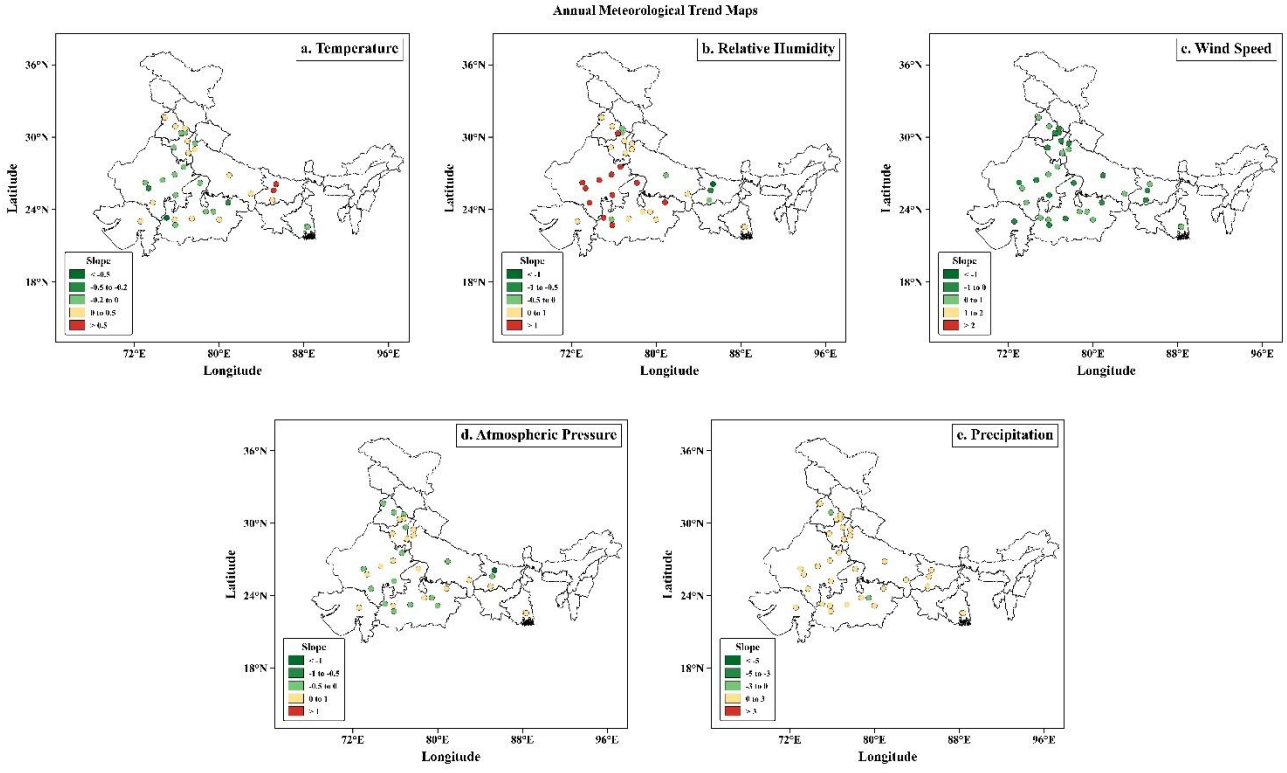

Figure 5. *Variation trends of meteorological elements at 37 cities from 2018 to 2025. A positive slope indicates the increase of meteorological elements (such as wind speed, temperature, precipitation, relatively humidity and atmospheric pressure), and vice versa. The greater the absolute value of the slope is, the faster the meteorological factor rises or falls).*

Annual trend maps of Temp, RH, WS, AP, and PPT reveal spatially coherent, variable-specific patterns of long-term change over 2018–2025. (**Figure 5).** Wind speed showed a predominantly declining trend at the majority of stations, particularly within the core NCR–western Uttar Pradesh–Haryana cluster, where dark- and mid-green markers (slope < -1.0 to -1.0–0 m s^{-1} yr^{-1}) dominate. A smaller subset of stations in Rajasthan and Madhya Pradesh showed weak positive (yellow, 0–1 m s^{-1} yr^{-1}) trends, but no station recorded a strong increasing trend (> 2 m s^{-1} yr^{-1}). Consistent with regional wind-stilling linked to urban surface roughness and aerosol-radiation feedbacks. Precipitation trends were generally weak and slightly positive across most of the domain, with the majority of stations falling in the 0–3 mm yr^{-1} class (yellow), and only isolated stations in western Rajasthan and central Madhya Pradesh showing a mild decline (-3 - 0 mm yr^{-1}, light green). There is no station with a significant positive (> 3 mm yr^{-1}) or negative (< -5 mm yr^{-1}) precipitation trend, indicating a fairly stable pattern of yearly precipitation in the region for the study period. The atmospheric pressure exhibited a varied pattern with a weekly declining to neutral trend dominating where green dots (declining, -1 to -0.5 hPa yr^{-1}) dominated the NCR region while yellow dots (increase 0 to 1 hPa/yr) were found in the peripheral and southern parts of the region. Most stations exhibited weakly positive (yellow, 0 to 0.5°C/yr) temperature trends while some stations in Rajasthan, Punjab, and Haryana showed weakly cooling (green, -0.2 to 0°C/yr) temperature trends. Notably, one or two stations in the eastern part of the domain (Bihar/Jharkhand region) recorded a markedly stronger warming trend (red, > 0.5 °C yr^{-1}), representing localized outliers against the otherwise gradual regional warming signal. Relative humidity showed the most spatially heterogeneous and pronounced trend of all five variables, with a striking cluster of strongly increasing (red, > 1% yr^{-1}) markers concentrated in the Punjab–Haryana–western Uttar Pradesh belt, in direct contrast to a smaller number of declining (green) stations further east and south. This spatial concentration of rising humidity in the northwestern IGP core is notable given its established negative correlation with particulate matter concentrations in prior studies, and may partly offset the air-quality benefits of the concurrent wind-speed decline described above.

3.3.2 Seasonal meteorological trends

As shown in **Figure S6,** Season-resolved maps (Pre-monsoon: Plot 1; Monsoon: Plot 2; Post-monsoon: Plot 3; Winter: Plot 4) show the annual patterns are not uniform year-round, especially for humidity and temperature. Wind speed declined consistently across all four seasons with similar spatial footprint, indicating a year-round rather than season-specific phenomenon. Precipitation trends stayed weakly positive across seasons, with monsoon map (**Figure S6- *Plot* 2b**) showing marginally more increase, as expected given it holds most of the annual rainfall signal. Atmospheric pressure trends were broadly stable across seasons, with a persistent NCR-core decline slightly more pronounced in post-monsoon map (**Figure S6- *Plot* 3c**). Temperature showed the clearest seasonal contrast: winter panel (**Figure S6- *Plot* 4d**) alone showed a red (>0.5°C/yr) marker plus wider warming spread, indicating faster winter warming — consistent with known preferential winter warming over northern India. Relative humidity showed the strongest seasonal signal: the Punjab–Haryana–western UP red cluster (>1%/yr) appeared in winter, pre-monsoon, and post-monsoon maps (**Figure S6- *Plot* 4e, *Plot* 2e, *Plot* 3e**) but was notably visibly less extensive during Monsoon (**Figure S6- *Plot* 2e**), meaning the long-term humidity rise is concentrated in the drier months, the same months with the highest PM levels, reinforcing a plausible link between rising humidity and cold-season pollution via reduced dispersion and hygroscopic aerosol growth. The summary is given in **Table 3** and **Table 4**.

Table 3. Qualitative summary of dominant meteorological trend classes by season, North India (2018–2025)

Variable	Annual	Winter	Pre-monsoon	Monsoon	Post-monsoon
Temperature	Weak warming; 1–2 strong outliers (east)	Weak–moderate warming; strongest of all	Weak warming	Weak warming	Weak warming

Variable	Annual	Winter	Pre-monsoon	Monsoon	Post-monsoon
		seasons			
Relative Humidity	Strong increase (Punjab–Haryana–West.UP cluster)	Strong increase (most extensive)	Strong increase	Weaker / more mixed	Strong increase
Wind Speed	Declining (core NCR)	Declining	Declining	Declining	Declining
Atmospheric Pressure	Weak decline (core) / neutral (periphery)	Weak decline	Weak decline	Weak decline	Weak decline (largest cluster)
Precipitation	Weak increase	Weak increase	Weak increase	Weak increase (strongest)	Weak increase

Table 4. Comparative summary: dominant meteorological drivers of $PM_{2.5}$/PM_{10} seasonality

Season	Wind Speed trend	RH trend	Implication for PM levels
Winter	Declining	Strongly increasing	Reduced dispersion + humidity-enhanced aerosol growth → highest PM (consistent with Section 3.3.2 findings)
Post-monsoon	Declining	Strongly increasing	Same mechanism; compounded by stubble-burning emissions
Pre-monsoon	Declining	Increasing (moderate)	Intermediate PM levels
Monsoon	Declining	Weakest increase	Wet scavenging dominates; lowest PM levels despite declining wind speed

3.4 Impact of Meteorological Conditions on $PM_{2.5}$ and PM_{10}

A cross-sectional fixed-effects panel regression estimated $PM_{2.5}$/PM_{10} as functions of Temp, RH, WS, AP, and PPT using monthly station-level data (2018–2025; 38 stations annual, 36–38 seasonal).

3.4.1 Annual Analysis

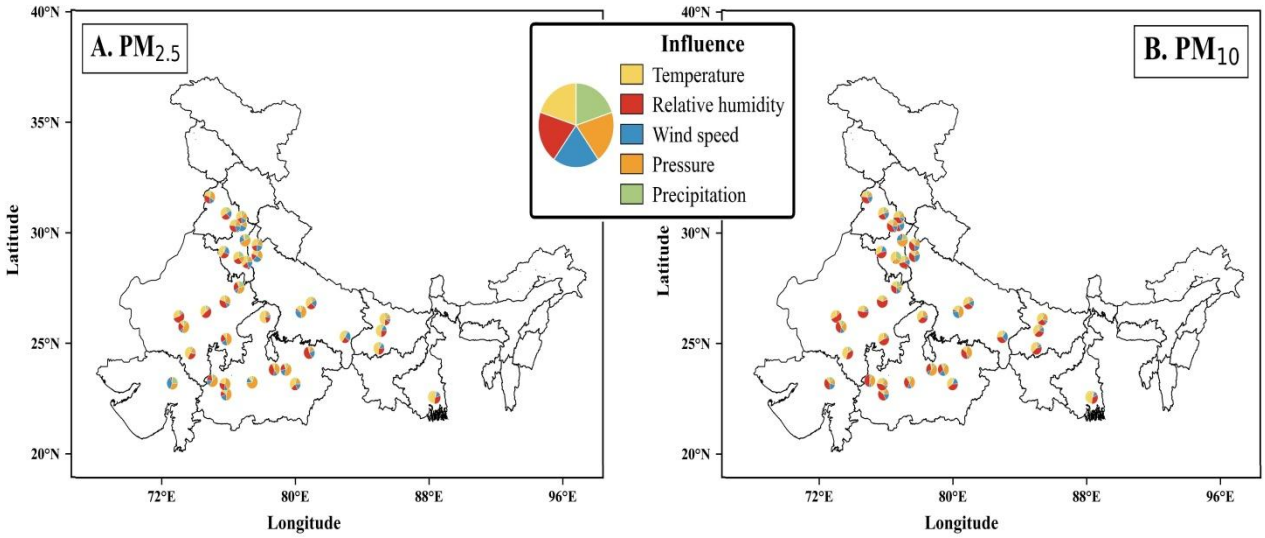

Figure 6. *MLR model results for 37 North Indian cities.*

In the MLR model for the annual analysis (**Figure 6**), the dependent variables are the concentrations of two air pollutants, while the independent variables comprise average wind speed, average temperature, precipitation, relative humidity, and average atmospheric pressure. The annual model explained moderate variance (R^2 = 0.201 $PM_{2.5}$; 0.214 PM_{10}; n = 71,514, 38 stations), in line with comparable regional MLR studies (R^2 = 0.19–0.93). All five variables (**Table 5**) were significant ($p < 0.01$). Wind speed was negatively associated with both pollutants ($PM_{2.5}$: -2.672 $\mu g/m^3$; PM_{10}: -3.838 $\mu g/m^3$ per m/s) - an order of magnitude stronger than typical large-scale panel estimates (-0.155/-0.220), reflecting the IGP's more confined airshed. Precipitation was also negative ($PM_{2.5}$: -0.762; PM_{10}: -1.476), consistent with wet scavenging. Pressure was positively associated with both ($PM_{2.5}$: +1.090; PM_{10}: +1.397), reflecting stable high-pressure conditions favoring accumulation. Temperature was negative ($PM_{2.5}$: -1.374; PM_{10}: -2.388), consistent with deeper mixing layers under warmer conditions. Humidity was negative annually ($PM_{2.5}$: -0.391; PM_{10}: -1.375) and, by standardized coefficients, the strongest single PM10 predictor (β = -0.339) ahead of temperature (β = -0.212) and wind speed (β = -0.093), while temperature remained dominant for $PM_{2.5}$ (β = -0.218) as shown in **Figure 6.**

Table 5. Estimated results of the annual (2018–2025, all-years-combined) panel regression of meteorological elements on $PM_{2.5}$ and PM_{10} concentrations across North India.

Variable	$PM_{2.5}$ (Unstd.)	PM_{10} (Unstd.)	$PM_{2.5}$ (β)	PM_{10} (β)
Wind speed	-2.672***	-3.838***	-0.116***	-0.093***
Precipitation	-0.762***	-1.476***	-0.068***	-0.074***
Atm. pressure	1.090***	1.397***	0.192***	0.137***
Temperature	-1.374***	-2.388***	-0.218***	-0.212***
Rel. humidity	-0.391***	-1.375***	-0.173***	-0.339***
Constant	-977.170***	-1129.830***	—	—
Obs / Sites	71,514 / 38	71,514 / 38	—	—
R^2	0.201	0.214	—	—

3.4.2 Seasonal Analysis

In the MLR model for seasonal analysis (**Figure S7**), the independent variables are average wind speed, average temperature, precipitation, relative humidity, and average atmospheric pressure, and the dependent variable is the concentration of two air pollutants. The data used in the model includes the monthly value of pollutant concentration and meteorological elements of 37 cities from 2018 to 2025.The F-test was used to test the significance of the model, and the t-test was used to test the significance of independent variables and *R*2 to judge the fitting effect of the model.

Season-specific models show meteorological drivers vary sharply by season (**Table S3**), masking heterogeneity in the pooled annual model - paralleling prior findings that autumn/winter PM meteorology correlations exceed spring/summer. Winter showed the strongest meteorological control overall: wind speed ($PM_{2.5}$: -4.042; PM_{10}: -6.331) and precipitation ($PM_{2.5}$: -4.546; PM_{10}: -8.004) had their largest effects, reflecting the shallow, stagnant winter boundary layer. Notably,

humidity reversed sign, becoming positively associated with $PM_{2.5}$ (+0.582, β = 0.178, largest winter coefficient) and PM_{10} (+0.140) suggesting winter humidity promotes hygroscopic growth rather than removal. Temperature lost significance for $PM_{2.5}$ ($p > 0.10$) and PM_{10}. Post-monsoon showed the second-strongest effects, with wind speed ($PM_{2.5}$: -4.043; PM_{10}: -6.985) and precipitation ($PM_{2.5}$: -2.310; PM_{10}: -4.625) again dominant; pressure and temperature retained annual-scale signs - consistent with post-monsoon being a peak-pollution season compounded by stubble burning. Pre-monsoon showed weaker explanatory power (R^2 = 0.049 $PM_{2.5}$; 0.119 PM_{10}), with precipitation the strongest standardized driver (β = -0.051/-0.072); temperature switched to positive ($PM_{2.5}$: +0.720; PM_{10}: +0.872), likely reflecting dust storms and thermal re-suspension of crustal material. Monsoon showed the weakest, most inconsistent signal: wind speed significant only for $PM_{2.5}$ (-0.313); precipitation non-significant for both (likely due to uniformly high, saturating rainfall); pressure significant only for PM_{10} (-0.329, the only season with a negative AP sign); temperature reversed to its strongest positive effect of any season ($PM_{2.5}$: +1.212; PM_{10}: +0.852). Humidity remained negative ($PM_{2.5}$: -0.397; PM_{10}: -1.634 - the largest-magnitude seasonal RH coefficient for PM_{10}), consistent with active wet-scavenging rather than winter-style hygroscopic growth.

The opposite/negative sign (**Table 6**) of the humidity in winter season, being positive instead of the negative that plays a consistent role elsewhere, directly accounts for excessive winter levels of PM, and corresponds geographically with areas experiencing maximum increases in humidity over the long term (Punjab-Haryana-western UP) where winter levels of $PM_{2.5}$/PM_{10} are also the highest.

Table 6. Summary of the dominant (largest standardized-coefficient) meteorological driver of $PM_{2.5}$ and PM_{10} concentration, by season.

Season	Dominant driver - $PM_{2.5}$	Dominant driver - PM_{10}	Sign
Annual	Temperature (β = −0.218)	Rel. humidity (β = −0.339)	Negative

Season	Dominant driver - $PM_{2.5}$	Dominant driver - PM_{10}	Sign
Winter	Rel. humidity (β = +0.178)	Wind speed (β = −0.121)	Positive (RH) / Negative (WS)
Post-monsoon	Temperature (β = −0.204)	Wind speed (β = −0.107)	Negative
Pre-monsoon	Rel. humidity (β = −0.112)	Rel. humidity (β = −0.264)	Negative
Monsoon	Rel. humidity (β = −0.290)	Rel. humidity (β = −0.493)	Negative

3.5 Pearson Correlation between PM and Meteorological Variables

Zero-order Pearson correlations were computed between $PM_{2.5}$, PM_{10}, and the five meteorological variables, annually and by season, using pooled daily data (2018–2025), to examine bivariate associations independent of the panel model's fixed effects.

3.5.1 Annual Correlation

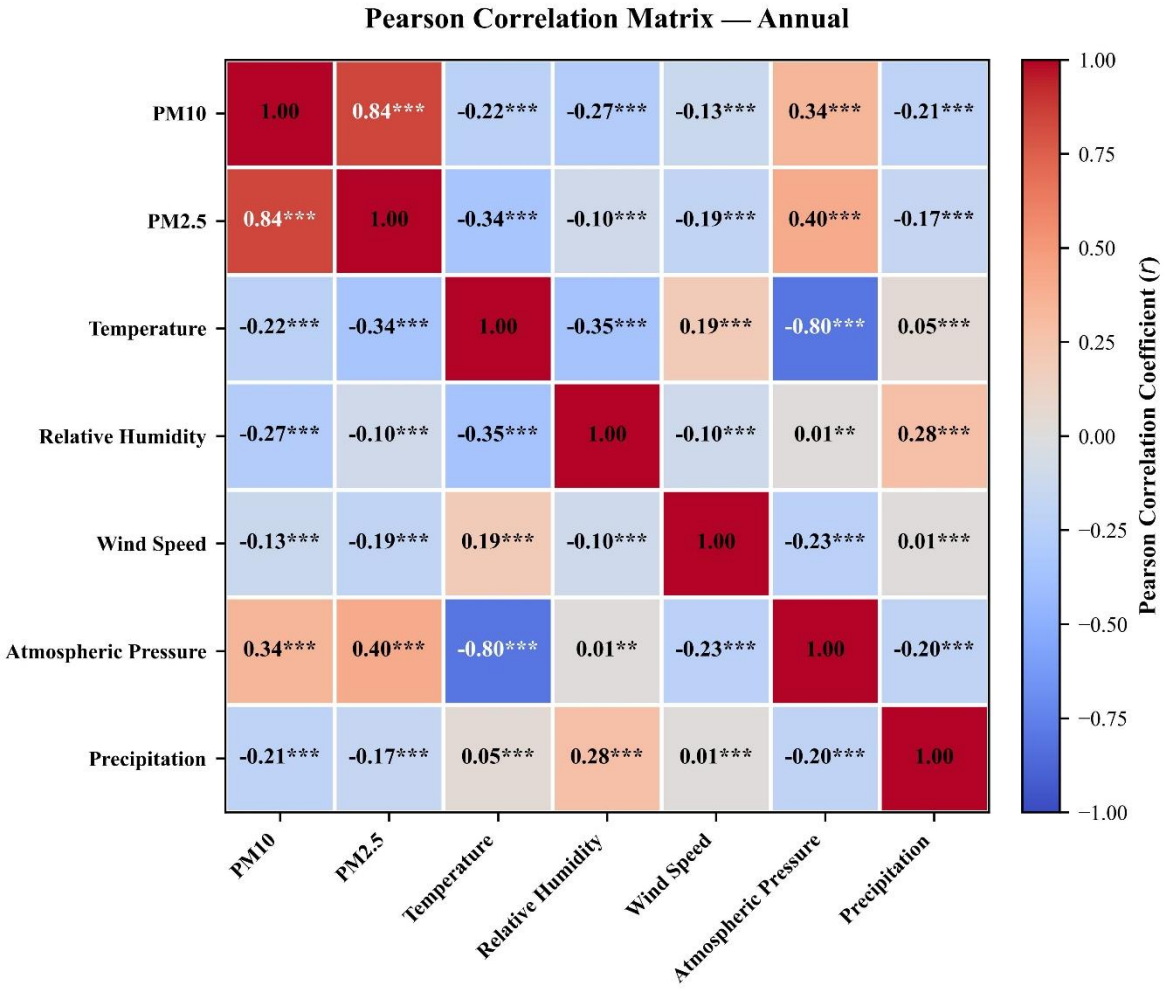

Figure 7. *Annual Pearson correlations, pollutants vs. meteorological factors.*

At the annual scale (**Figure 7, Table 7),** $PM_{2.5}$ and PM_{10} were strongly correlated ($r = 0.84$, $p < 0.001$), confirming shared sources/dispersion. Both showed significant negative correlation with wind speed ($PM_{2.5}$: -0.19; PM_{10}: -0.13) and precipitation ($PM_{2.5}$: -0.17; PM_{10}: -0.21). Pressure showed the strongest positive correlation with $PM_{2.5}$ of any variable ($r = 0.40$) and a strong one with PM_{10} ($r = 0.34$). Temperature was negative for both ($PM_{2.5}$: -0.34; PM_{10}: -0.22); humidity was weakly negative for PM_{10} (-0.27) and weaker still for $PM_{2.5}$ (-0.10) annually masking a seasonal reversal detailed below. Among meteorological variables, pressure and temperature were strongly anti-correlated ($r = -0.80$), matching the panel-regression finding that AP and Tem act oppositely on PM.

3.6.2 Seasonal Correlation structure

As shown in Table 7, Winter showed the strongest $PM_{2.5}$ - PM_{10} coupling ($r = 0.84$) but weakest meteorological control: wind and precipitation retained expected signs but weaker magnitude, pressure was near-zero, and humidity reversed to positive for $PM_{2.5}$ ($r = +0.16$) matching the regression reversal and reinforcing that winter humidity promotes hygroscopic growth rather than removal. Temperature–humidity correlation was also strongest here ($r = -0.54$), reflecting cold, humid, fog-prone winter conditions. Pre-monsoon differed sharply: temperature turned positive for both pollutants ($PM_{2.5}$: +0.15; PM_{10}: +0.24), consistent with dust-storm and re-suspension effects; humidity stayed negative ($PM_{2.5}$: -0.18; PM_{10}: -0.33); pressure turned weakly negative ($-0.07/-0.14$), reversing its annual/post-monsoon positive relationship. Monsoon had the weakest $PM_{2.5}$ - PM_{10} coupling of all seasons ($r = 0.71$) and most distinctive pattern: temperature showed its strongest positive correlation of any season ($PM_{2.5}$: +0.41; PM_{10}: +0.47), while humidity showed its strongest negative correlation ($PM_{2.5}$: -0.43; PM_{10}: -0.54) opposite the winter pattern consistent with humidity being tied to active rainfall/scavenging (temperature–humidity anti-correlation $r = -0.84$, strongest of any season). Wind speed showed negligible or weak positive correlation with PM_{10}

584 (+0.05), suggesting minor dispersion control during monsoon. Post-monsoon showed the strongest
585 $PM_{2.5}$ - PM_{10} coupling of all (r = 0.87), closely mirroring the annual pattern, with a strong positive
586 pressure correlation ($PM_{2.5}$: 0.27; PM_{10}: 0.25), the second-highest after annual consistent with onset
587 of stable, winter-like high-pressure conditions compounded by stubble burning.
588
589 **Table 7. Pearson correlation coefficients (r) between $PM_{2.5}$/PM_{10} and meteorological variables,**
590 **annual and by season, North India (2018–2025).**

Season	PM_{10}–$PM_{2.5}$	PM–WS	PM–Pre	PM–AP	PM–Temp	PM–RH
Annual	0.84***	−0.19/−0.13	−0.17/−0.21	0.40/0.34	−0.34/−0.22	−0.10/−0.27
Winter	0.84***	−0.15/−0.13	−0.08/−0.11	0.02/−0.02	−0.08/−0.01	+0.16/+0.02
Pre-monsoon	0.75***	−0.09/−0.02	−0.09/−0.15	−0.07/−0.14	+0.15/+0.24	−0.18/−0.33
Monsoon	0.71***	−0.01/+0.05	−0.14/−0.18	−0.07/−0.10	+0.41/+0.47	−0.43/−0.54
Post-monsoon	0.87***	−0.14/−0.13	−0.13/−0.16	0.27/0.25	−0.27/−0.24	−0.09/−0.19

591 *Notes: All correlations significant at $p < 0.001$ unless otherwise indicated. Values shown as*
592 *$PM_{2.5}$/PM_{10} where two figures are given. Bold values highlight the most notable seasonal reversals*
593 *discussed in text.*
594
595 Across all four seasons, the $PM_{2.5}$–PM_{10} correlation as shown in ***Figure S8*** remained consistently
596 strong (r = 0.71–0.87), confirming shared source and dispersion controls, but was weakest during
597 monsoon and strongest during post-monsoon, reflecting the greater relative influence of localized
598 wet-deposition variability during the rainy season. The most policy-relevant finding is the sign
599 reversal of relative humidity between winter (positive) and monsoon (strongly negative), and the
600 corresponding reversal of temperature between winter/post-monsoon (negative) and pre-
601 monsoon/monsoon (positive) - together indicating that no single meteorological variable exerts a
602 consistent, season-independent control on particulate concentrations in North India. This finding,
603 consistent with both the panel regression results (**Section 3.4.2**) and the reference literature's

observation that autumn/winter meteorological correlations with particulate matter are typically stronger than in spring/summer, underscores the necessity of season-specific rather than pooled annual meteorological analysis when developing air quality forecasting or early-warning systems for the region.

Table 8. Synthesis of Seasonal $PM_{2.5}$–PM_{10} Coupling and Meteorological Control Patterns

Season	$PM_{2.5}$–PM_{10} Correlation (r)	Relative Humidity Relationship	Temperature Relationship	Interpretation
Winter	0.84	Positive (reversal)	Negative	RH reversal drives elevated winter PM via hygroscopic aerosol growth
Pre-monsoon	0.75	Negative	Positive (reversal)	Temperature reversal linked to dust-storm re-suspension
Monsoon	0.71 (weakest)	Strongly negative	Positive (reversal)	RH tied to active wet scavenging rather than aerosol growth
Post-monsoon	0.87 (strongest)	Negative	Negative	Pattern closely mirrors annual-scale relationships

Table 9. Key Points — Seasonal PM–Meteorology Coupling

Finding	Detail
$PM_{2.5}$–PM_{10} coupling range	r = 0.71–0.87 across all seasons — confirms shared source and dispersion controls
Weakest coupling	Monsoon - reflects greater influence of localized wet-deposition variability
Strongest coupling	Post-monsoon
RH sign reversal	Winter (positive) vs. Monsoon (strongly negative)
Temperature sign reversal	Winter/Post-monsoon (negative) vs. Pre-monsoon/Monsoon (positive)
Consistency with regression	Matches panel regression results
Consistency with literature	Aligns with reference literature showing stronger autumn/winter PM–meteorology correlations than spring/summer
Policy implication	No single meteorological variable shows consistent, season-independent control on PM - supports season-specific rather than pooled annual analysis for air quality forecasting/early-warning systems

Table 8 summarizes the seasonal synthesis of $PM_{2.5}$–PM_{10} coupling and meteorological control patterns. The $PM_{2.5}$–PM_{10} correlation remained consistently strong across all seasons (r = 0.71–0.87), weakest in monsoon and strongest in post-monsoon. The most policy-relevant finding is the sign reversal of relative humidity and temperature across seasons, indicating that no single meteorological variable exerts consistent, season-independent control over particulate concentrations in North India emphasising the need for season-specific rather than pooled meteorological analysis in regional air quality forecasting. Seasonal PM–meteorology coupling (**Table 9**) analysis was conducted to identify variations in pollutant–meteorological relationships that may be masked by annual analysis. The strong $PM_{2.5}$–PM_{10} correlation (r = 0.71–0.87), along with seasonal changes in the effects of humidity and temperature, indicates that meteorological controls vary across seasons. These findings, consistent with the regression results, support the use of season-specific analysis for improved interpretation and air-quality forecasting.

4. Conclusion

This study presents a comprehensive spatio-temporal analysis of PM_{10} and $PM_{2.5}$ across 81 cities in northern India (2018–2025), integrating Sen's slope estimation, the Mann–Kendall test, panel regression, and Pearson correlation to characterize both the magnitude and statistical reliability of particulate trends and their meteorological drivers across the IGP.

1. Despite mitigation efforts, the 81-city multi-year mean (PM_{10}: 130.0 μg/m^3; $PM_{2.5}$: 62.7 μg/m^3) exceeds NAAQS/WHO limits by factor of 2.2–8.7, with pollution sharply clustered in NCR hotspots (Greater Noida, Ghaziabad, Bhiwadi, Noida) and secondary hotspots along the Varanasi–Kanpur corridor and Haryana, while peripheral MP/Gujarat towns remain far cleaner.
2. Post-monsoon is the most polluted season (PM_{10}: 172.1 μg/m^3; $PM_{2.5}$: 90.0 μg/m^3), closely followed by winter, with pre-monsoon intermediate and monsoon roughly 50% lower driven

by stagnant winter atmospheric conditions and stubble burning versus monsoon wet scavenging.

3. Sen's slope analysis shows median declines in both PM_{10} (-2.3 $\mu g/m^3/yr$) and $PM_{2.5}$ (-1.5 $\mu g/m^3/yr$), led by UP cities, plausibly reflecting NCAP, PMUY, and BS-VI interventions yet 32.1% of cities (mostly Haryana/Punjab) show rising $PM_{2.5}$, flagging emerging sources needing attention.
4. Mann–Kendall tests confirm significant declines in 27.2% of cities for $PM_{2.5}$ and 22.5% for PM_{10} (versus almost no significant increases), with these declines clustering in UP, MP, and Rajasthan largely matching NCAP priority zones and concentrated in winter and post-monsoon.
5. Wind speed, precipitation, pressure, temperature, and humidity are all significant annual-scale drivers (R^2 = 0.201–0.214), with strong $PM_{2.5}$–PM_{10} coupling (r = 0.84), but relative humidity the strongest single annual PM_{10} predictor — reverses sign in winter, switching from a dispersing to an aggravating influence via hygroscopic aerosol growth.
6. Both relative humidity and temperature show seasonal sign reversals (e.g., temperature negative in winter/post-monsoon but positive in pre-monsoon/monsoon due to dust re-suspension and convective mixing), demonstrating that no single meteorological variable controls PM concentrations consistently year-round.

Acknowledgement

All authors gratefully acknowledge Amity University, Noida, Uttar Pradesh, for providing the facilities and support. The authors are thankful to India Meteorological Department (IMD), Ministry of Earth Sciences (MoES), Govt of India for providing institutional support and research facility for conducting this study. The authors also sincerely thank the Central Pollution Control Board (CPCB) for providing the monitoring data essential for this study. CPCB's continued commitment to environmental monitoring has been invaluable in enabling the analysis and interpretation presented in this research.

Author Contributions

Gaurav Singh: Conceptualization, Writing-original draft, Software, Formal analysis, Investigation. **M.P. Raju**: Visualization, Formal analysis, Writing-original draft, Supervision. **V.K. Soni**: Investigation, Formal analysis, Supervision**. Chinmay Jena**: Formal analysis, Supervision. **Suman Gurja**: Formal analysis, Supervision.

Funding Declaration

This research did not receive any specific grant from funding agencies in the public, commercial, or not-for-profit sectors.

Availability of Data and Materials

The data that support the findings of this study are available from the corresponding author on reasonable request.

Conflict of Interest

The authors have no competing interests to declare that are relevant to the content of this article.

Ethical standards

This study did not involve any experiments on humans or animals. Therefore, ethical approval and informed consent were not required.

References

Balakrishnan K et al (2019) The impact of air pollution on deaths, disease burden, and life expectancy across the states of India: the Global Burden of Disease Study 2017. Lancet Planet Health 3(1):e26–e39

Bhawan P, Nagar EA (2020) Central Pollution Control Board. Central Pollution Control Board, New Delhi, India, Technical Report, pp 20–21

Cao J, Chow JC, Lee FSC, Watson JG (2013) Evolution of PM2.5 measurements and standards in the U.S. and future perspectives for China. Aerosol Air Qual Res 13:1197–1211

Central Pollution Control Board (CPCB) (2019) National Clean Air Programme (NCAP). Ministry of Environment, Forest and Climate Change, Government of India

Central Pollution Control Board/Centre for Research on Energy and Clean Air (CREA) (2026) Tracing the hazy air 2026: progress report on the National Clean Air Programme (NCAP)

Chatterjee A, Raul S et al (2025) Satellite-based long-term assessment of particulate matter trends across the Indo-Gangetic Plain, Himalayan region, and North-East India (2000–2024). Atmos Environ (in press)

Commission for Air Quality Management in NCR and Adjoining Areas (CAQM) (2023) Annual report on air quality management in the National Capital Region and adjoining areas. Ministry of Environment, Forest and Climate Change, Government of India, New Delhi

David LM, Ravishankara AR, Kodros JK, Pierce JR, Venkataraman C, Sadavarte P (2019) Premature mortality due to PM2.5 over India: effect of atmospheric transport and anthropogenic emissions. GeoHealth 3:2–10

Di D, Zhang L, Wu X, Leng R (2020) Long-term exposure to outdoor air pollution and the risk of development of rheumatoid arthritis: a systematic review and meta-analysis. Semin Arthritis Rheum 50(2)

Dumka UC, Kaskaoutis DG, Srivastava MK, Devara PCS (2021) Dust and anthropogenic contributions to aerosol optical depth and radiative forcing over the Indo-Gangetic Plain. Sci Total Environ 745:140966

Guo Q, He Z, Wang Z (2023) Predicting daily PM2.5 concentration employing wavelet artificial neural networks based on meteorological elements in Shanghai, China. Toxics 11

Guo Q, He Z, Wang Z (2024) Monthly climate prediction using deep convolutional neural network and long short-term memory. Sci Rep 14:17748

Guttikunda SK, Gurjar BR (2012) Role of meteorology, emission sources, and land use in PM2.5 chemistry and premature mortality in Delhi, India. Environ Sci Technol 46(8):4327–4335

He Z, Guo Q, Wang Z, Li X (2022) Prediction of monthly PM2.5 concentration in Liaocheng in China employing artificial neural network. Atmosphere 13

Hirsch RM, Slack JR, Smith RA (1982) Techniques of trend analysis for monthly water quality data. Water Resour Res 18(1):107–121

ICIMOD (2024) Millions of people across the Indo-Gangetic Plain and Himalayan foothills continue to breathe hazardous air. International Centre for Integrated Mountain Development, Kathmandu

Jena C, Ghude SD, Kumar R, Debnath S, Govardhan G, Soni VK, Kulkarni SH, Beig G, Nanjundiah RS, Rajeevan M (2021) Performance of high resolution (400 m) PM2.5 forecast over Delhi. Sci Rep 11:4104

Kamyotra J, Saha D, Tyagi SK, Sen AK, Srivastava RC, Pathak A (2011) Guidelines for the measurement of ambient air pollutants. Central Pollution Control Board, Ministry of Environment & Forests, Government of India

Kendall MG (1975) Rank correlation methods, 4th edn. Charles Griffin, London

Krishna B, Balakrishnan K, Siddiqui AR, Begum BA, Bachani D, Brauer M (2017) Tackling the health burden of air pollution in South Asia. BMJ 359:j5209

Kumar A, Singh N, Ansari TA, Solanki R (2021) PM10 and PM2.5 in the Indo-Gangetic Plain (IGP) of India: chemical characterization, source analysis, and transport pathways. Environ Adv 6:100120

Kumar M, Tiwari S, Murari V, Singh AK, Banerjee T (2015) Wintertime characteristics of aerosols at middle Indo-Gangetic Plain: impacts of regional meteorology and long-range transport. Atmos Environ 104:162–175

Kumar RP, Perumpully SJ, Samuel C, Gautam S (2022) Exposure and health: a progress update by evaluation and scientometric analysis. Stoch Environ Res Risk Assess 37(2):453–465

Kumar V, Sahu SK, Mishra K, Bhangare RC (2018) 18-year ambient PM2.5 exposure and night light trends in Indian cities. Aerosol Air Qual Res 18(10):2682–2693

Kuttippurath J, Patel VK, Singh A (2022) India's air pollution burden (2019–2023): spatial–temporal trends, emissions, weather effects, and adult health risks across state and city. Water Air Soil Pollut 237(3):368

Lakra K, Avishek K (2024) Influence of meteorological variables and air pollutants on fog/smog formation in seven major cities of the Indo-Gangetic Plain. Environ Monit Assess 196(6):533

Landrigan PJ (2017) Air pollution and health. Lancet Public Health 2(1):e4–e5

Mani SA, Mani FS, Kumar A, Shah S, Peltier RE (2020) Traffic-related PM. Transp Res Part D Transp Environ 87

Mann HB (1945) Nonparametric tests against trend. Econometrica 13(3):245–259

Mohammad L, Bandyopadhyay J, Mondal I, Altuwaijri HA, Hossain SA, Juliev M, Almaliki AH (2025) Air pollution and respiratory health risks in Jharkhand: a remote sensing and statistical approach. Environ Monit Assess 197(5):540

Naskar S, Majumder S, Biswas B (2025) Assessment of Air Pollution Index (API) using FAHP and correlations between PM10 and Sentinel-5P (TROPOMI) AOD of Jharkhand, India. Environ Sci Pollut Res 32:5102–5118

Ngo NS, Asseko SVJ, Ebanega MO, Allo'o Allo'o SM, Hystad P (2019) The relationship among PM2.5, traffic emissions, and socioeconomic status: evidence from Gabon using low-cost, portable air quality monitors. Transp Res Part D Transp Environ 68:2–9

Patel VK, Kuttippurath J, Kashyap R (2022) Spatiotemporal variability and source attribution of PM2.5/PM10 ratios: aerosol type classification and AQI evaluation across seventy monitoring stations in Delhi and Haryana, India. Atmos Pollut Res 13(6):101462

Paulot F, Naik V, Horowitz LW (2022) Reduction in near-surface wind speeds with increasing CO2 may worsen winter air quality in the Indo-Gangetic Plain. Geophys Res Lett 49(18):e2022GL099039

Ramadan MNA, Ali MAH, Jaber H, Alkhedher M (2025) Blockchain-secured IoT-federated learning for industrial air pollution monitoring: a mechanistic approach to exposure prediction and environmental safety. Ecotoxicol Environ Saf 300:118442

Raul S, Chatterjee A (2025) Trajectory analysis of PM transport pathways from the Indo-Gangetic Plain to the Himalayas: a 25-year satellite perspective. Environ Res Lett 20(4):045012

Sen PK (1968) Estimates of the regression coefficient based on Kendall's tau. J Am Stat Assoc 63(324):1379–1389

Sharma G, Gupta M, Gargava P, Kota SH (2024) Mapping air quality trends across 336 cities in India: insights from three decades of monitoring (1987–2019). Environ Int 191:108979

Sharma N, Kumar R, Malyan V, Choudhary A (2025) Spatiotemporal variability and source attribution of PM2.5/PM10 ratios across seventy monitoring stations in Delhi and Haryana, India. Sci Total Environ 924:171598

Sharma S, Zhang M, Gao J, Zhang H, Kota SH (2021) Effect of restricted emissions during COVID-19 on air quality in India. Sci Total Environ 728:138878

Shi Y, Matsunaga T, Yamaguchi Y, Li Z, Gu X, Chen X (2018) Long-term trends and spatial patterns of satellite-retrieved PM2.5 concentrations in South and Southeast Asia from 1999 to 2014. Sci Total Environ 615:177–186

Singh A, Banerjee T, Srivastava A (2022) Very high particulate pollution over northwest India captured by a high-density in situ sensor network during the post-monsoon season. npj Clim Atmos Sci 6:108

Srivastava AK, Misra S, Dwivedi AK, Tiwari S, Bisht DS, Srivastava MK, Dey S (2014) Aerosol optical depth and chemical mass closure in the Indo-Gangetic Basin. Atmos Res 138:203–213

Theil H (1950) A rank-invariant method of linear and polynomial regression analysis. Proc K Ned Akad Wet 53:386–392

Venkatesan P (2016) WHO report: air pollution is a major threat to health. Lancet Respir Med 4(5):351

Wei J, Liu S, Li Z, Cribb M (2024) Improved daily PM2.5 estimates in India reveal inequalities in recent enhancement of air quality. Sci Adv 10(28):eadq1071

World Bank (2022) The global health cost of PM2.5 air pollution: a case for action beyond 2021. International Development in Focus. World Bank, Washington, DC

World Health Organization (WHO) (2021) WHO global air quality guidelines: particulate matter (PM2.5 and PM10), ozone, nitrogen dioxide, sulfur dioxide and carbon monoxide. World Health Organization, Geneva

World Health Organization (WHO) (2022) Air pollution. World Health Organization, Geneva

Xie Y, Zhou M, Hunt KMR, Mauzerall DL (2024) Recent PM2.5 air quality improvements in India benefited from meteorological variation. Nat Sustain 7:983–993

Yue S, Pilon P, Phinney B, Cavadias G (2002) The influence of autocorrelation on the ability to detect trend in hydrological series. Hydrol Process 16(9):1807–1829

Zhong H, Xu R, Lu H, Liu Y, Zhu M (2023) Dynamic assessment of population exposure to traffic-originated PM2.5 based on multisource geo-spatial data. Transp Res Part D Transp Environ 124:103923

Supplementary Files

This is a list of supplementary files associated with this preprint. Click to download.

- SupplementaryMaterial.docx